Assessment of Stability of Slopes under Drawdown Conditions

By P. A. Lane[1] and D. V. Griffiths,[2] Member, ASCE

Abstract: The traditional approach for estimating the stability of slopes under different submergence conditions is the charts of Morgernstern and, more recently, proprietary computer programs, both utilizing limit-state analyses. The chart approach is limited by geometry and material property considerations and the limit-state approach by assumptions about analysis method and failure mechanism. The finite-element method offers a powerful method for analyzing complex geometries and properties of slope stability problems, but may be unattractive for routine use by supervisory staff. By comparison a chart based approach is useful, particularly when setting operating conditions on, for example, drawdown rates for dams and reservoirs. This paper seeks to explore the use of the finite-element method to produce operating charts for such circumstances that should be applicable to real structures.

INTRODUCTION

The stability of a slope depends on its geometry, its material properties, and the forces to which it is subjected. These forces include the effects of water both internally, in the form of pore-water pressures and seepage forces, and externally, in terms of hydrostatic and hydrodynamic effects. The effect of water on slope stability can be seen by considering the slope under different degrees of submergence and drawdown. The implications of this were first quantified by Morgernstern (1963) and later investigated by, for example, Desai (1977) and Cousins (1978). All used limit-state analyses for the estimation of the factor of safety (FOS) of the slope under a range of conditions to produce a series of charts for practicing engineers to utilize.

The finite-element program FE-EMB1 developed by Griffiths (1996) has been extended to FE-EMB1LG by Lane and Griffiths (1997) to include any combination of submergence and drawdown conditions and to allow for the automatic generation of pore-water pressures or the insertion of known values for both prediction and back-analysis. The program utilizes the power of the finite-element method to account for potentially complex geometries and material properties, but is used here to develop a chart based approach for the operation of dams and reservoirs to minimize the risk of slope failure under drawdown conditions.

BRIEF DESCRIPTION OF FINITE-ELEMENT MODEL

The finite-element program is for 2D, plane strain, slope stability analysis by finite elements using eight-node quadrilateral elements of elastic-visco-plastic soil with a Mohr-Coulomb failure criterion and a nonassociated flow rule. The primary development has been the inclusion of free-surface and/or external reservoir loading. The soil's self-weight is modeled by a gravity "turn-on" procedure (Smith and Griffiths 1988) with nodal loads added in a single increment.

The FOS for the slope is defined by division of the original shear strength parameters c', ϕ' to give their values at failure, c'_f, ϕ'_f where

$$c'_f = c'/\text{FOS} \tag{1}$$

$$\phi'_f = \arctan\left(\frac{\tan\phi'}{\text{FOS}}\right) \tag{2}$$

There are several possible definitions of failure, for example, (1) some test of bulging of the slope profile (Snitbhan and Chen 1976); (2) limiting of the shear stresses on the potential failure surface (Duncan and Dunlop 1969); or (3) nonconvergence of the solution (Zienkiewicz and Taylor 1989). These are discussed in Abramson et al. (1995) from the original paper by Wong (1984), but without resolution. In the examples studied here the nonconvergence option coupled with a sudden increase in nodal displacements is taken as being a suitable indicator of failure.

When the algorithm cannot converge within a user-specified maximum number of iterations, the implication is that no stress distribution can be found that is simultaneously able to satisfy both the Mohr-Coulomb failure criterion and global equilibrium. If the algorithm is unable to satisfy these criteria, failure is said to have occurred. Slope failure and numerical nonconvergence occur simultaneously and are accompanied by a dramatic increase in the nodal displacements within the mesh. Most of the results shown in this paper used an iteration ceiling of 500 and are based on a graph of FOS versus $E'\delta_{max}/\gamma H^2$ (a dimensionless displacement), where δ_{max} is the maximum nodal displacement at convergence and H is the height of the slope of unit weight and effective Young's Modulus E′. This graph may be used alongside the displaced mesh and vector plots to indicate both the FOS and the nature of the failure mechanism. In comparison, the FOS generated by traditional methods represents the ratio between the driving and restoring forces, but this is essentially the same definition of FOS as used in the finite-element approach.

The program produces graphical output to illustrate the mechanism of failure. To emphasize the mechanism of failure the iterations limit may be increased to 1,000 and the plotted displacement vectors limited to above a scaled minimum in order to differentiate the mechanism from the background mesh. Similarly, the plots of displaced mesh have been produced by allowing the higher iterations limit in order to emphasize the mechanism. In some cases this appears to give a highly distorted mesh, but this effect is occurring long past when failure has been established numerically, and is purely a visual effect, not influencing the identified FOS.

Fig. 1 shows the mesh for a simple, dry 2:1 slope with properties of $\phi' = 40°$, $c' = 1$ kN/m^2; and $D = 1.0$ (Smith and Griffiths 1988), where D is the depth to a firm layer. In this case $D = H$, the height of the slope. With a unit weight of 20 kN/m^3, the FOS for the slope under its own self-weight can be found using the gravity turn-on procedure. The displacement vector plot in Fig. 2 shows a simple rotational failure,

[1]Lect., Geotechnics Res. Group, Dept. of Civ. and Struct. Engrg., UMIST, Manchester M60 1QD, U.K.

[2]Prof., Geomechanics Res. Ctr., Colorado School of Mines, Golden, CO 80401.

Note. Discussion open until October 1, 2000. To extend the closing date one month, a written request must be filed with the ASCE Manager of Journals. The manuscript for this paper was submitted for review and possible publication on November 16, 1998. This paper is part of the ***Journal of Geotechnical and Geoenvironmental Engineering***, Vol. 126, No. 5, May, 2000. ©ASCE, ISSN 1090-0241/00/0005-0443–0450/$8.00 + $.50 per page. Paper No. 19604.

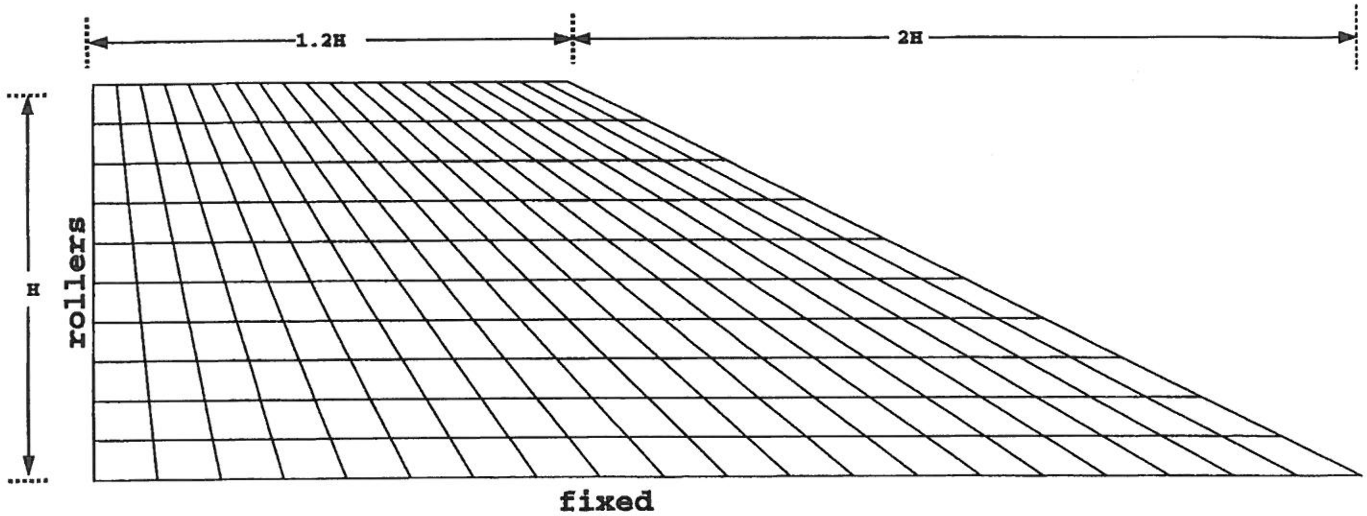

FIG. 1. Initial Mesh for 2:1 Homogeneous Slope: $\phi' = 40°$; $c'/\gamma H = 0.05$; $D = 1.0$

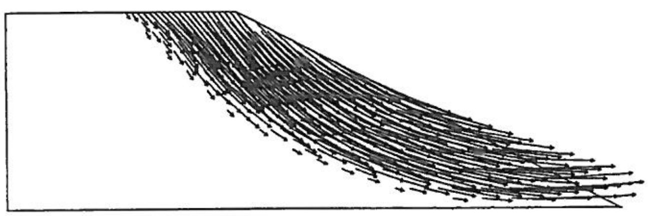

FIG. 2. Displacement Vectors at Failure for 2:1 Homogeneous Slope: $\phi' = 40°$; $c'/\gamma H = 0.05$, $D = 1.0$

as expected, with a FOS of 2.5, i.e., the slope fails under its own self-weight when its effective cohesion c' and its internal angle of friction in the form tan ϕ' have been factored by 2.5. The program has been validated for a range of slopes with different dimensions and properties and excellent agreement is obtained with the charts of Bishop and Morgernstern (1960).

STABILITY UNDER PARTIAL SUBMERGENCE

The strength of a soil, in terms of its ability to resist applied loading, is a function of its effective stress state. This, in turn, depends on the pore-water pressure at each point. Pore-water pressures may be derived from historical conditions (especially in fine-grained materials) or measured in current conditions (usually in coarse-grained materials). When the excess pore pressures generated by changes in loading take a "long" period of time to dissipate, the problem is said to be undrained. When the dissipation is "rapid," it is said to be drained.

The definition of long is not absolute but invariably means that the rate of dissipation of excess pore pressures is many times less than the rate of change of the loading condition. The stability of simple slopes with variable internal pore pressures was extensively studied by Bishop and Morgernstern (1960) whose charts are commonly used in classical limit-state

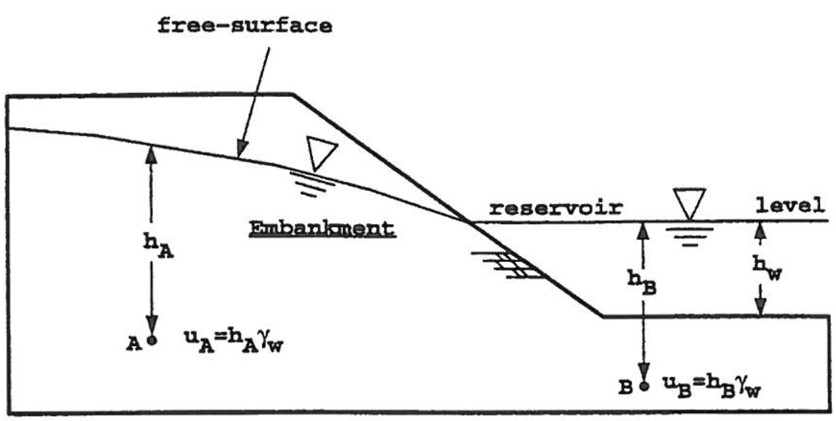

FIG. 3. Slope with Free Surface and Reservoir Loading

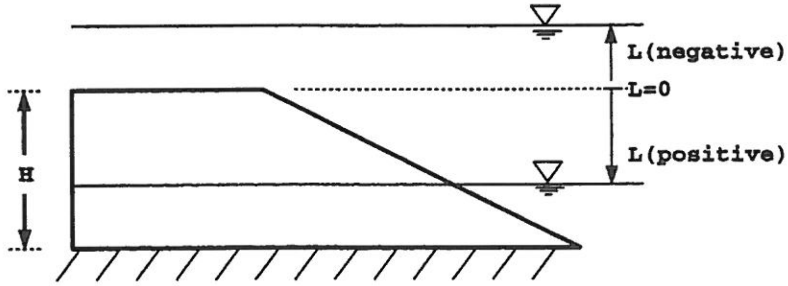

FIG. 4. Slow Drawdown Problem. Homogeneous 2:1 Slope with Horizontal Free Surface (above and below Free Surface): $\phi' = 20°$; $c'/\gamma H = 0.05$; $D = 1.0$

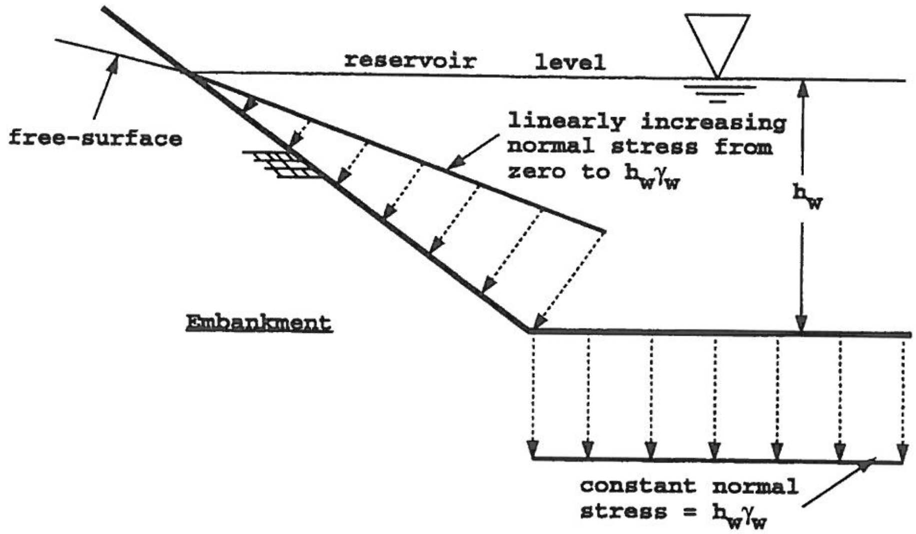

FIG. 5. Detail of Submerged Area of Slope Beneath Free-Standing Reservoir Water, Showing Stresses to be Applied to Surface of Mesh as Equivalent Nodal Loads

analyses. More recently Lambe and D'Silva (1995) have reported on the importance of correct modeling of internal pore-water pressures. The effect of seepage was considered by Desai (1977), and this is discussed later in this paper.

The program has been fully validated in modeling pore-water pressures both directly and indirectly such as through the pore pressure ratio r_u or as hydrostatic values from a free surface. Fig. 3 illustrates some general definitions of internal free-surface, reservoir level and hydrostatic pore-water pressures for a partially submerged slope. This paper is primarily concerned with the analysis of slope stability under either (1) rapid drawdown, when the internal section of the free surface is horizontal and at the level immediately prior to drawdown of the reservoir level; or (2) slow drawdown or partial submergence, where the internal section of the free surface has stabilized to the new reservoir level. These two levels are shown in Fig. 4. For these extreme cases the piezometric and phreatic surfaces are coincident, with horizontal flowlines except on the slope face itself. The intermediate seepage case, where flowlines are sloping or curved, is considered alongside results presented by Desai (1977).

The effective-stress condition also depends on the total stress, which is usually derived from the soil's total self-weight plus any applied loading. In the case of a submerged slope, the water provides a linearly increasing normal hydrostatic pressure on the embankment face. In this case the pressure on the face is computed simply as the weight of water vertically above. Fig. 5 illustrates the arrangements to represent the loading on the slope under partial submergence.

Partial submergence can also be regarded as a case of slow drawdown in that it is assumed that the pore-water pressures have time to adjust to the partially submerged water level, i.e., that the internal free-water level in the slope equalizes to the reservoir level at any time. The effects of seepage have been neglected for the purposes of this paper. The drawdown ratio L/H is the ratio of the depth by which the water falls L to the height of the slope H.

Fig. 4 shows a 2:1 slope with a horizontal free surface at a depth L below the crest. Using the method described above, the FOS of the slope has been computed for several different values of the drawdown ratio L/H that has been varied from -0.2 (slope completely submerged with the water level $0.2H$ above the crest) to 1.0 (water level at the base of the slope). A constant total unit weight of 20 kN/m^3 has been assigned to the entire slope, both above and below the water level, although this could be altered to reflect the draining of slope material about the free surface if required.

Fig. 6 shows the results from the finite-element program for partial submergence or slow drawdown of this slope. It gives a minimum FOS of about 1.3 when the drawdown ratio L/H is about 0.7 (the reservoir level is at about 30% of the slope height). For comparison, the case has been analyzed both by finite elements and by a traditional limit equilibrium computer package (*SLOPE* 1985) using Bishop's method (Bishop 1955). There is excellent agreement between the results from the two approaches over the full range. The results of Bishop and Morgernstern (1960) and Morgernstern (1963), which correspond to the fully drained and fully submerged cases, are also shown giving excellent agreement.

A possible explanation of the observed minimum is due to the cohesive strength of the slope (which is unaffected by buoyancy) and the trade-off between soil weight and soil shear strength as the drawdown level is varied. In the initial stages of drawdown ($L/H < 0.7$), the increased weight of the slope has a proportionately greater destabilizing effect than the increased frictional strength and the FOS falls. At higher drawdown levels ($L/H > 0.7$), however, the increased frictional strength starts to have a greater influence than the increased weight and the FOS rises. Other results of this type have been reported by Lane and Griffiths (1997) for a slope which was stable (FOS > 1) when "dry" or fully submerged, but became unstable (FOS < 1) at a critical value, typically 70%, of the drawdown ratio L/H.

It should also be noted from the horizontal part of the graph in Fig. 6, corresponding to $L/H \leq 0$, that the FOS for a fully submerged slope is unaffected by the depth of water above the crest. It is thus possible for a slope to be stable when fully submerged and when fully drained, but to be unstable in a partially submerged condition. Partial submergence was analyzed by Cousins (1978) to produce a set of charts that are for homogeneous cases only. The results shown here agree well with Cousins, but the finite-element approach may also be extended to inhomogeneous conditions.

The possible influence of cohesion has been considered for a range of $c'/(\gamma H)$ from 0.01 to 1.0 and for ϕ' from 12 to 40°, and a selection of these are given in Fig. 7. All combinations indicate that the observed minimum FOS occurs at a drawdown ratio between 0.2 and 0.3.

STABILITY UNDER FULL RAPID DRAWDOWN

The results presented so far illustrate the case of partial submergence or drawdown at a rate slow enough for the internal free surface and the reservoir level to equalize effectively at

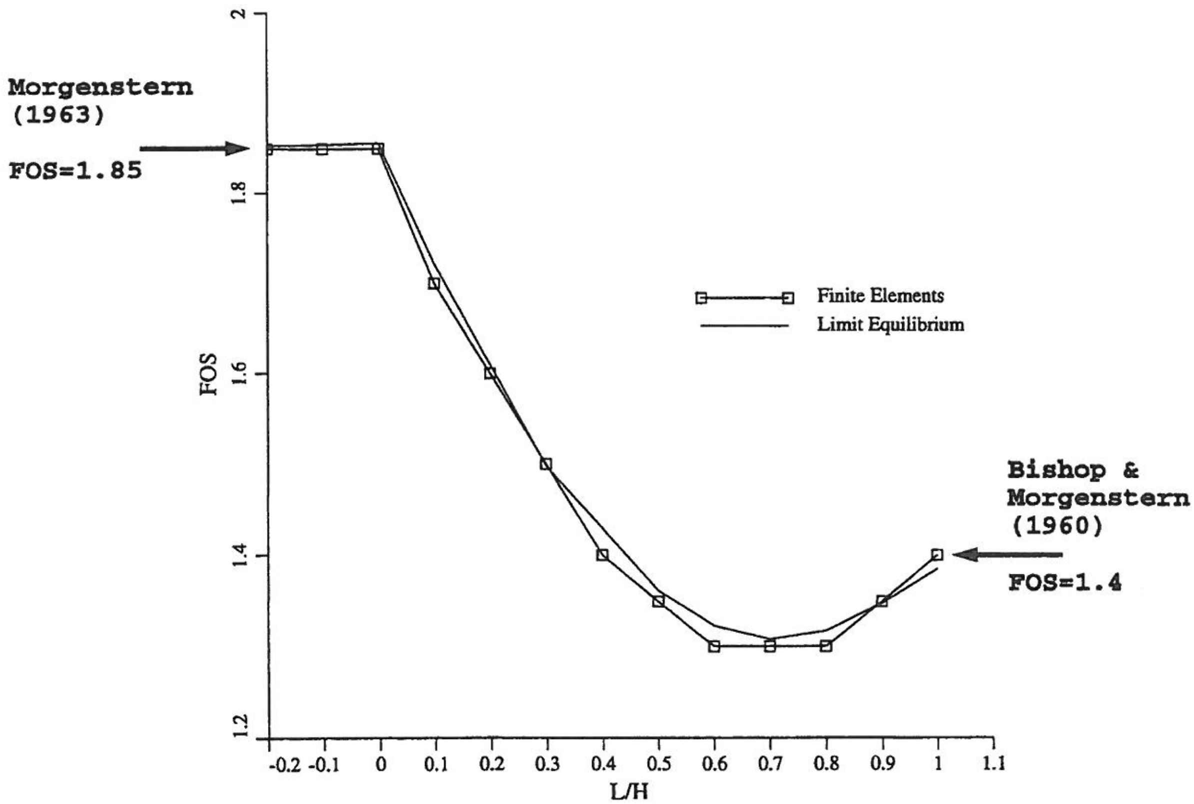

FIG. 6. FOS in Slow Drawdown Problem for Different Values of Drawdown Ratio L/H (above and below Free Surface): $\phi' = 20°$; $c'/\gamma H = 0.05$; $D = 1.0$

any point. The most critical condition for many submerged slopes is the rapid drawdown case. If the reservoir level is reduced over a "short" time in a fine-grained material the internal pore-water pressures continue to reflect the original water level for some time after drawdown. But the stabilizing effect of the reservoir water loading is lost.

Morgernstern (1963) presented stability charts based on parametric studies using limit-state analyses where it is assumed that pore-water pressures were based on the free-water surface level, neglecting seepage, and that no dissipation occurred during drawdown. This means that the piezometric surface, causing the pore-water pressures within the embankment, remains unchanged. In the finite-element program rapid drawdown is modeled when the piezometric surface is specified as per the original water level, but the face loads are based on the drawndown reservoir level, which in this case is below that of the piezometric values.

Morgernstern's charts are nondimensional for various values of effective cohesion c', unit weight γ and slope height H using the parameter

$$\frac{c'}{\gamma H} \tag{3}$$

Interpolation can be used between the published values. A significant consideration in relation to this paper is that all slopes analyzed by Morgernstern (1963) are assumed to be initially fully submerged ($L = 0$), and it is pointed out in the 1963 paper that the charts do not automatically give the minimum FOS for a partial drawdown ($L/H < 1.0$) case. Morgenstern's results are based on a circular failure surface tangential to the base of the slope. In this instance, the case for a failure circle passing above the slope base must be checked separately, as this may give a lower result than for a failure tangential to the base. The finite-element program does not suffer this disadvantage and automatically identifies the most critical failure mechanism, irrespective of the drawdown ratio. A comparison of results between Morgernstern and the finite-element program is shown in Fig. 8 for a range of cases. Excellent agreement was obtained, with the finite-element results slightly lower, especially over the higher drawdown ratios.

Desai (1977) also considered the case of stability under drawdown at differing rates using a numerical approach to locate the internal free surface followed by a limit-state analysis for the subsequent FOS estimation. A range of drawdown rates relative to the slopes' material permeability were considered but it was concluded that this was of secondary importance. This would suggest that seepage is of secondary importance in modeling this form of collapse. His results can be considered as semirapid drawdown in that they are faster than for equalization to be complete, but they are slower than for rapid drawdown. Desai estimated that the difference in the FOS between his analysis and for rapid drawdown would be a reduction of the order of 2–8%.

Fig. 9 shows a comparison of the results of Desai (for semirapid drawdown) and for those of Morgernstern and the finite-element program (both for rapid drawdown). These suggest that the impact of the rapid condition is greater than Desai estimated—up to 40% in some cases. There is some inconsistency in Desai's results for $\phi' = 25°$ for the particular case of a 2:1 slope that may be contributing to this difference. The final graph in Fig. 9 of Desai's paper, for a 2:1 slope, appears to be out of line with the pattern of the other results in Figs. 6–9 and suggests a higher result than would be expected. This may be exaggerating the differential identified here.

DRAWDOWN FROM PARTIAL SUBMERGENCE

Morgernstern (1963) assumes drawdown is from the case of full submergence. But, as has been shown, a partially submerged slope may have a lower initial FOS and therefore could be at greater risk of a potential failure with drawdown from this partially submerged condition. The charts of Morgernstern, Desai, and Cousins provide no direct method of analyzing this case. For the 2:1 slope the cases of slow draw-

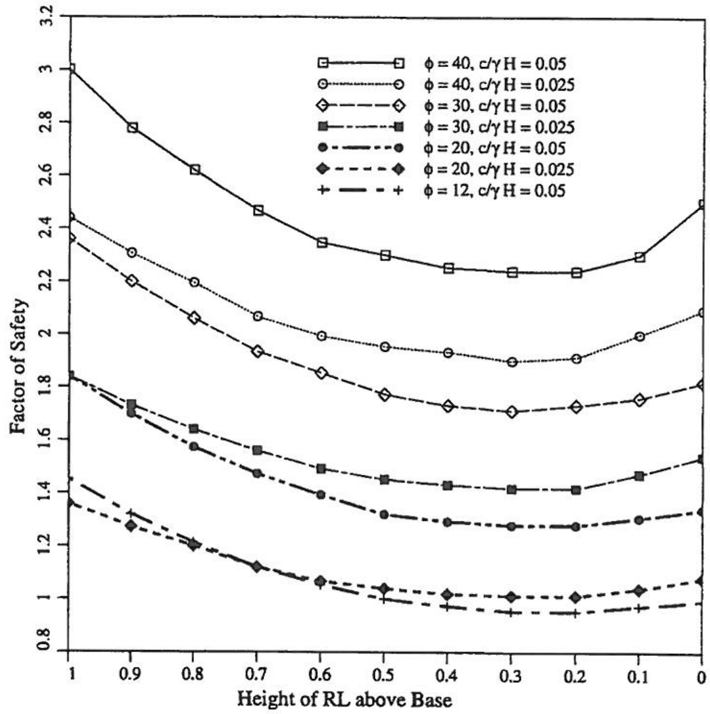

FIG. 7. Minimum FOS for Rapid Drawdown Conditions for 2:1 Slope: ϕ = 12, 20, 30, 40°; $c'/\gamma H$ = 0.025, 0.05; D = 1.0

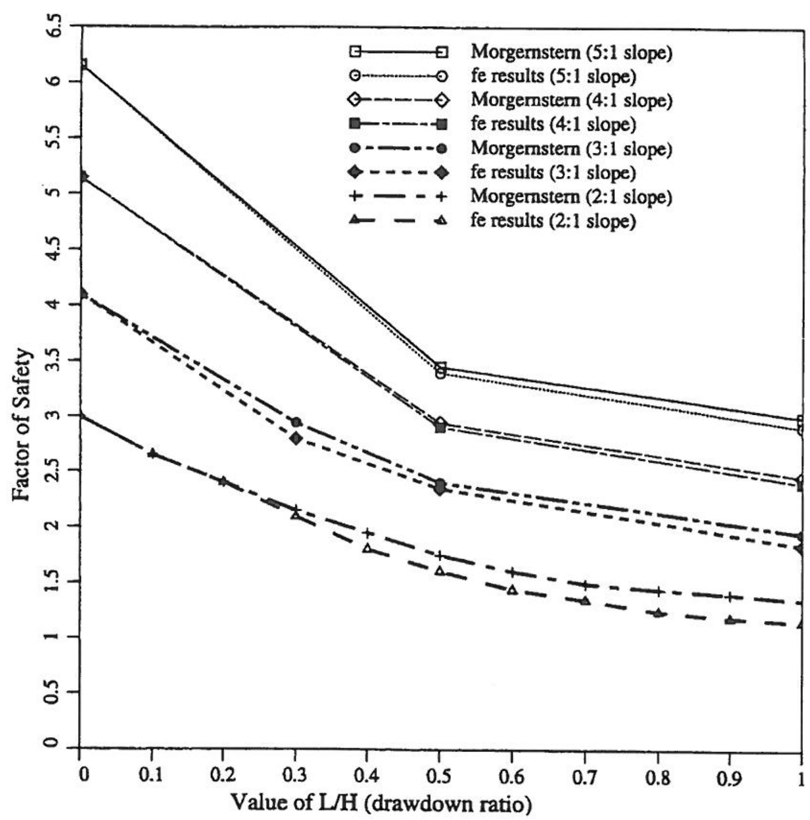

FIG. 8. Comparison of Morgensterm and Finite-Element Results for Rapid Drawdown Conditions for 2:1 Slope: ϕ = 40°; $c'/\gamma H$ = 0.05; D = 1.0

down (or partial submergence), rapid drawdown from full submergence, and rapid drawdown from partial submergence are considered. The results are shown in Fig. 10, for $\phi' = 40°$, using the mesh shown in Fig. 1.

The FOS at full submergence ($L/H = 0$) is 3.0 (Point A in Fig. 10). The slow drawdown from full height (or partially submerged) condition is shown (Curve i). This reaches a minimum of about 2.24 at a drawdown ratio of 70% (Point B). As drawdown continues the FOS rises and, if drawdown were complete ($L/H = 1.0$), the FOS of 2.51 is that for a dry slope (Point C).

When rapid drawdown from full submergence (Curve ii) is considered then the FOS drops rapidly from the fully submerged value (starting at Point A) to a minimum at complete rapid drawdown of 1.15 (Point D). For the final curve [Curve iii] of Fig. 10, the case of rapid drawdown from partial sub-

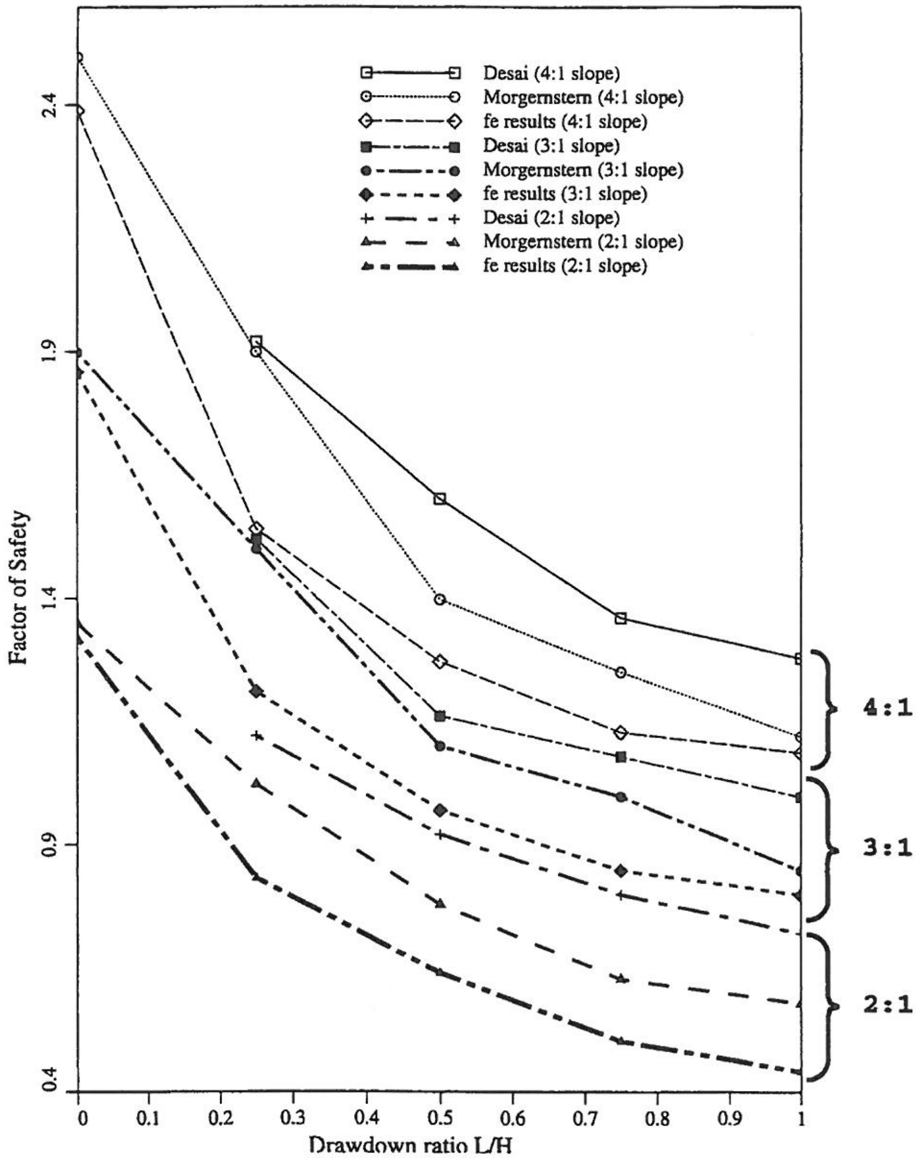

FIG. 9. Comparison of Desai, Morgenstern, and Finite-Element Results for Rapid Drawdown Conditions for 2:1 Slope: $\phi = 25°$, $c'/\gamma H = 0.0125$, $D = 1.0$

mergence is considered. For this case the drawdown is complete in that the reservoir level falls from an initial drawdown ratio value (L/H) to the base. So, for example, if the reservoir level were initially at L/H of 0.7 (i.e., at 30% H), the FOS would be about 2.24 (Point B) in this partially submerged condition. If the reservoir were then to be drawn down rapidly from this height, the FOS would fall to about 1.90 (Point E).

If the fully submerged slope (initial FOS of 3.0 at Point A) were rapidly drawn down to a drawdown ratio of 0.2, this operation would reduce the FOS to about 2.40 (Point F). Over time the internal free surface would stabilize at 80% of the slope height and the FOS would rise to 2.62 (Point G) in the partially submerged state. However, if from 80% submergence it were then to be fully drawn down from $L/H = 0.2$ to $L/H = 0$, the FOS would fall to about 1.24 (Point H).

Note that in Curve iii, the rapid drawdown from partial submergence, has the same terminating FOS (at Point D′) of 1.15 as the rapid drawdown to partial submergence Curve ii at Point D. This is because they represent the same case of 100% rapid drawdown from full submergence.

OPERATING CHARTS AND PROCEDURES

When considering drawdown conditions for a submerged slope, a lower FOS is temporarily acceptable, which differs from normal working conditions. The minimum acceptable FOS may be defined and then the chart for a particular slope utilized to determine the drawdown procedure to keep above that minimum. Fig. 11 shows the chart for a 2:1 slope with $\phi = 20°$.

Assuming a minimum FOS of 1.2 might be acceptable under rapid drawdown, and starting from a fully submerged condition (Point A) it would be possible to draw the reservoir level down to 70% of the slope height (a drawdown ratio of about 0.3) rapidly (using Curve ii) to Point B. This would take it to the minimum FOS of about 1.2. (Full drawdown would result in collapse at about 50% drawdown). The slope could then be left to recover until the internal free surface was at or about reservoir level (of 70% H), and the FOS would rise to about 1.44 over time (Point C). Utilizing the slow drawdown curve, the reservoir level could be lowered to a drawdown ratio of about 0.76 (a reservoir level of about 24% of the slope height), giving a FOS of 1.28 at Point D. From this partially submerged condition the level could then be drawn down rapidly to empty with an FOS of about 1.20 (utilizing Curve iii, Point E). Thus the minimum FOS is never violated but the drawdown would be faster than under slow conditions throughout.

This process illustrates the usefulness of potential charts

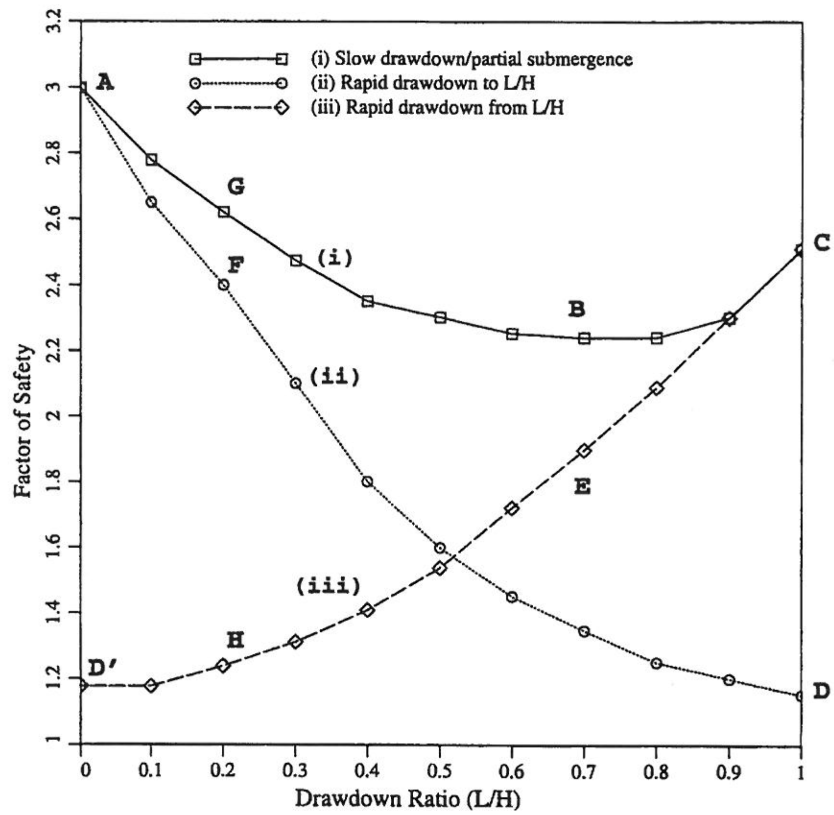

FIG. 10. Comparison of FOS for Different Drawdown Conditions for 2:1 Slope: $\phi' = 40°$; $c'/\gamma H = 0.05$; $D = 1.0$

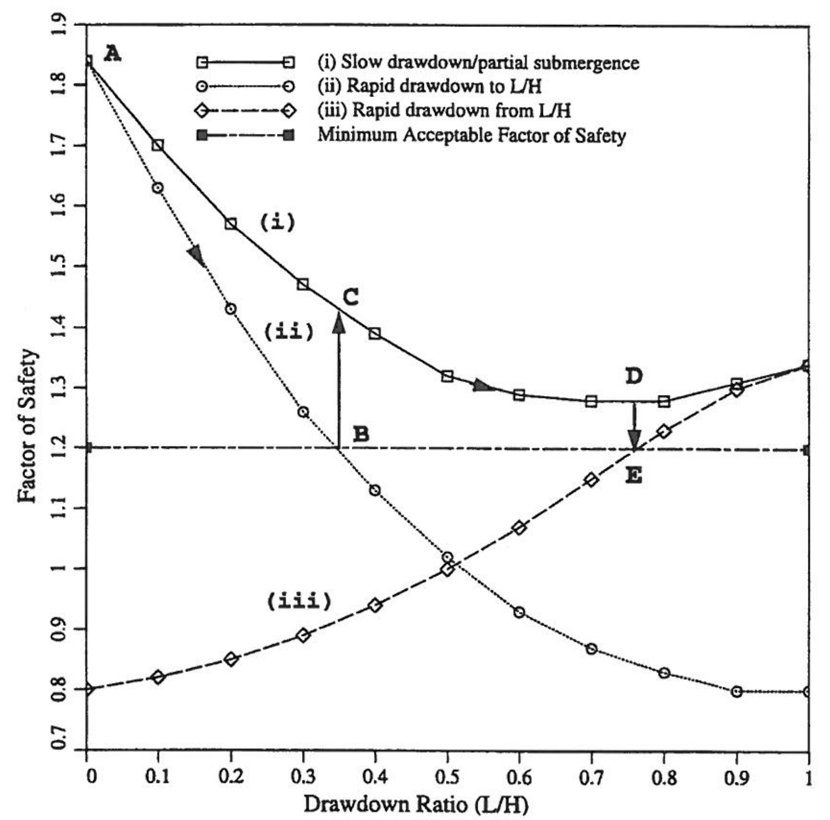

FIG. 11. Operation of Charts for Drawdown Conditions for 2:1 Slope: $\phi' = 20°$; $c'/\gamma H = 0.05$; $D = 1.0$

based on rapid drawdown from partial submergence. The process may be summarized as follows:

1. A minimum acceptable FOS is selected for the drawdown operation.
2. Starting from full submergence level (Point A) the rapid drawdown ratio corresponding to the minimum FOS is identified. If on examining Curve ii full rapid drawdown is not possible, the drawdown is taken to the level corresponding to the acceptable FOS (Point A to Point B)

along Curve ii and held there until equalization has occurred (Point B to Point C).

3. Utilizing Curve iii for rapid drawdown from partial submergence, the partial submergence level corresponding to the minimum FOS is identified (Point E), and the point corresponding to this drawdown ratio on Curve i is identified (Point D).
4. Slow drawdown is carried out between the drawdown level in Step 2 and the level identified in Step 3 (Point C to Point D) along Curve i.
5. Once slow drawdown from Step 4 is complete, rapid drawdown can be completed (Point D to Point E).

If the slope is initially partially submerged, the process starts at some position along the slow drawdown Curve i (i.e., from Step 3, Point C). This would be a conservative assumption in terms of the FOS as Curve ii assumes drawdown from full submergence.

If the drawdown is for <100% drawdown, Curve ii is examined first to see if this can be done rapidly without violating the minimum FOS. If this cannot be done, the process follows Steps 1–4, terminating at Point D. In a real structure, if the permeability is known or can be estimated from observations of the rate of change of water levels under drawdown conditions, it is possible to control the rate of the slow section of the drawdown (Points C–D in the process) to maintain the minimum FOS required. The results presented here proscribe limits to the rate of drawdown where the permeabilities may not be known with sufficient accuracy in a potentially multimaterial structure and will always produce a workable estimate of permitted drawdown levels and rate.

These steps illustrate the use of the charts that, once produced, are suitable for use by supervisory staff in normal operations. The examples considered here were for homogeneous cases, but the finite-element method is not constrained to this and should therefore be applicable to real structures.

CONCLUDING REMARKS

In analyzing a slope with varying submergence levels, it is common for the engineer to consider rapid drawdown as a potentially critical condition. Starting from a condition of full submergence, different drawdown ratios may be considered until the lowest acceptable FOS is found. Drawdown of the reservoir might then be programmed to minimize the risk of failure by allowing staged drawdown to interim, partially submerged conditions. However, it may be tempting for the engineer then to assume that full drawdown could be completed from some interim stage. The results shown here show that this is not necessarily a safe assumption.

Similarly, it is rare in practice for a slope to be fully submerged, e.g., an earth dam reservoir would not be expected to be at full submergence for all except flood conditions. The charts of Morgernstern (1963) and Cousins (1978) do not provide a direct method of estimating the FOS in the case of rapid drawdown from partial submergence. The finite-element method can identify critical cases not readily accessible with the traditional methods of analysis and without a priori assumption of the mode of failure.

The finite-element method has been used to identify critical cases of partial submergence and rapid drawdown for partially submerged slopes. Traditional methods of analysis cannot cover the full range of possible critical conditions or adequately represent inhomogeneous slopes and complex loading arrangements. Thus, the finite-element method can perform a wider range of analysis than can be handled by traditional methods for all but the simplest submerged slope problems. Utilizing the finite-element method, potentially critical conditions of rapid drawdown from partial submergence have been identified and a chart based approach developed for operating safely.

ACKNOWLEDGMENTS

Dr. Lane was a visting assistant professor at the Colorado School of Mines, Golden, Colo., for the period of this research. Support is gratefully acknowledged to the Colorado School of Mines and to the Peter Allen Scholarship Fund of UMIST, Manchester, U.K. The support of the National Science Foundation, Washington, D.C. Grant No. CMS-9512434 is also acknowledged.

APPENDIX I. REFERENCES

Abramson, L. W., Lee, T. S., Sharma, S., and Boyce, G. M. (1995). *Slope stability and stabilization methods*. Wiley, New York.

Bishop, A. W. (1955). "The use of the slip circle in the stability analysis of slopes." *Géotechnique*, London, 5(1), 7–17.

Bishop, A. W., and Morgernstern, N. R. (1960). "Stability coefficients for earth slopes." *Géotechnique*, London, 10(1), 129–150.

Cousins, B. F. (1978). "Stability charts for simple earth slopes." *J. Geotech. Engrg. Div.*, ASCE, 104(2), 267–279.

Desai, C. S. (1977). "Drawdown analysis of slopes by numerical method." *J. Geotech. Engrg. Div.*, ASCE, 103(7), 667–676.

Duncan, J. M., and Dunlop, P. (1969). "Slopes in stiff fissured clays and soils." *J. Soil Mech. and Found. Div.*, ASCE, 95(5), 467–492.

Griffiths, D. V. (1996). "FE-EMB2 and FE-EMB1: Slope stability software by finite elements." *Geomechanics Res. Ctr. Rep. GRC-96-37*, Colorado School of Mines, Golden, Colo.

Lambe, T. W., and D'Silva, F. (1995). "The Bishop slope revisited." *Geotech. News*, 13(4), 49–55.

Lane, P. A., and Griffiths, D. V. (1997). "Finite element slope stability analysis—Why are engineers still drawing circles?" *Proc., 6th Int. Conf. Numer. Methods Geomech., NUMOG VI*, Balkema, Rotterdam, The Netherlands, 589–593.

Morgernstern, N. R. (1963). "Stability charts for earth slopes during rapid drawdown." *Géotechnique*, London, 13(1), 121–131.

SLOPE. (1985). Geosolve, London.

Smith, I. M., and Griffiths, D. V. (1988). *Programming the finite element method*, 2nd Ed., Wiley, Chichester, U.K.

Snitbhan, N., and Chen, W. F. (1976). "Elastic-plastic deformation analysis of soil slopes." *Comp. and Struct.*, 9, 567–577.

Wong, F. S. (1984). "Uncertainties in modeling of slope stability." *Comp. and Struct.*, 19, 777–791.

Zienkiewicz, O. C., and Taylor, R. L. (1989). *The finite element method, Vol. 1*, 4th Ed., McGraw-Hill, New York.

APPENDIX II. NOTATION

The following symbols are used in this paper:

c_f = effective soil cohesion at failure (kN/m^2);
D = depth factor;
E' = effective Young's Modulus (kN/m^2);
H = slope height (m);
L = reservoir level below slope crest (m);
RL = reservoir level above slope base (m);
r_u = pore water pressure ratio;
δ_{max} = maximum nodal displacement at non-convergence;
γ = unit weight of soil (kN/m^3); and
ϕ'_f = effective soil angle of friction at failure.